

2.

Aerodynamics and aero elasticity

2.1. Introduction

Aero elasticity is the discipline concerned with phenomena wherein the fluid (air) and structural motions interact significantly. The forces arising due to the structural motions in the fluid are called self-excited or aero elastic. Classified distinctly from these are the aerodynamic forces which appear because of the physical presence of the structure in the fluid (air) and are not dependent on structural motion.

Any civil engineering structure such as a long-span bridge or a tall building is viewed aerodynamically as a bluff body as opposed to a streamlined shape such as that of an airfoil. Bluff-body aero elasticity is quite different from airfoil or thin plate aero elasticity. For bluff objects of wind engineering applications, it has not to date been possible to develop expressions for the aerodynamic derivatives starting from basic fluid flow principles. However, according to Scanlan and Tomko [66], for small oscillations, the self-excited forces on a bluff body may be treated as linear in heave and pitch motions and their first two derivatives, being possible to measure the aerodynamic coefficients by means of specially designed wind tunnel tests. Flutter prediction for bridges with bluff cross sections is studied by Starossek [78].

The existing bridge state-of-the-art aero elastic response methodology owes its origin to the studies made earlier on airfoil or thin plate theory. Even today, these studies are useful regarding the format or type of results to be anticipated. As the spans of suspension bridges become ultra-long, the bridge cross sections tend to become more streamlined, and may be expected to resemble in their behavior to that of the airfoil or thin plate, which further emphasizes the importance of the latter in the present study.

The determination of the dynamic air forces acting on a flat plate or on an airfoil which oscillates vertically and torsionally in a steady air stream has been treated

by several authors in the past. Expressions for the air forces suitable for the following investigation were derived by Theodorsen [84], [85], [86], [87]. Equivalent equations have been developed independently by Kasner & Fingado [26] and by Kármán & Sears [24]. The Theodorsen solution is based on the assumption that the vibrating flat plate is infinitely thin and the air flow is two dimensional. Under the latter assumption, the equations apply only to cases where the object under wind action is sufficiently extended perpendicularly to the air flow so that the altered conditions at the ends influence the total effect of the air forces only to a negligible degree. This condition is satisfied to a large extent in the case of suspension bridges.

The Theodorsen equations were derived for small harmonic oscillations about the position of equilibrium, composed of simultaneous vertical and torsional vibrations of constant amplitudes. Consequently, they apply solely to the narrow zone of transition from stable to unstable motion, which may be considered a sustained harmonic oscillation of constant amplitude. Therefore, the Theodorsen expressions for the dynamic air forces suffice to solve the problem of self-excitation from its practical viewpoint - that is, the determination of the critical wind velocity and the characteristics of the motion at that wind speed.

2.2. Air forces acting on a vibrating flat plate

Consider a long flat plate having the width $B=2b$ and vibrating vertically and torsionally about its position of equilibrium, h being the vertical or bending amplitude of the point C , upward displacements being positive; α is the angle of rotation, the torsional amplitude, counted positive when the plate rotates clockwise. The air forces L and M are expressed as functions of the coordinates h , α and their derivatives with respect to time, see Figure 2-1. Forces L and M represent the unsteady (or self-excited) aerodynamic lift and moment about the rotation axis per unit length. At critical wind velocity v_c the two components of the coupled motion have the same frequency, but show a difference of their phase angles.

The force components in the vertical direction and around the longitudinal axis are represented by the air force vector F_L defined by two components:

$$F_L = \begin{bmatrix} -L \\ M \end{bmatrix} = \begin{bmatrix} L_1 + L_2 + L_3 \\ M_1 + \frac{b}{2}(L_1 - L_3) \end{bmatrix} \quad (2.1)$$

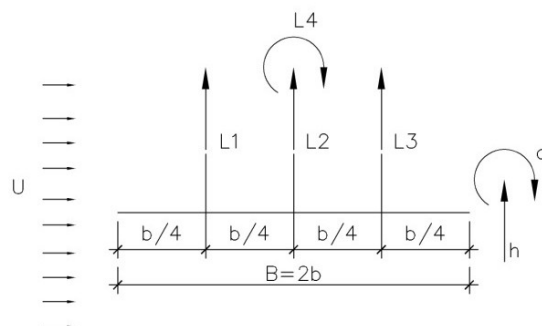


Figure 2-1– Force components experimented by a flat plate under wind flow.

in which

$$L_1 = 2\pi\rho b C(k) U \left(U\alpha + \dot{h} + \frac{b}{2}\dot{\alpha} \right) ; L_2 = \pi\rho b^2 \ddot{h} ; L_3 = \pi\rho b^2 U \dot{\alpha} \quad (2.2a)$$

$$M_1 = -\frac{\pi}{8} \rho b^4 \ddot{\alpha} \quad (2.2b)$$

The circulatory component of the lift force is represented by force L_1 , acting in the leading fourth of the bridge width B . L_2 and M_1 are the added aerodynamic masses in vertical and rotational directions, respectively, acting in the structure center of gravity. L_3 contains the non-circulatory component which results from the moment M . L_3 acts in the trailing fourth of the bridge width B , and represents the added aerodynamic mass and added rotational mass moment of inertia corresponding to the mass and rotational mass moment of inertia of the circumscribed air cylinder having the width B . These are negligible terms compared with the inertia force and moment of the vibrating structure, but will be included here for reasons of completeness.

Substituting expressions (2.2) in (2.1), one obtains:

$$\mathbf{F}_L = \begin{bmatrix} -L_1 \\ M_1 \end{bmatrix} = \begin{bmatrix} \pi\rho b^2 (U\dot{\alpha} + \ddot{h}) + 2\pi\rho U b C(k) (U\alpha + \dot{h} + b\dot{\alpha}/2) \\ -\pi\rho b^2 (bU\dot{\alpha}/2 + b^2\ddot{\alpha}/8) + \pi\rho U b^2 C(k) (U\alpha + \dot{h} + b\dot{\alpha}/2) \end{bmatrix} \quad (2.3)$$

where $C(k)$ is the Theodorsen function, defined as:

$$C(k) = F(k) + i G(k), \quad (2.4)$$

The variable $k = b\omega/U$ is defined as the reduced frequency, a dimensionless variable proportional to ω that can be regarded as a modified Strouhal number.

$F(k)$ and $G(k)$ are composed by Bessel functions of the first and second kind, $J_0(k)$, $J_1(k)$, $Y_0(k)$, $Y_1(k)$, respectively, $i = \sqrt{-1}$, ω is the circular frequency of oscillation of the airfoil, U is the mean wind velocity, b is the half-chord length of

the airfoil or half-width of the plate and ρ is the air density (1.225 kg/m³ in SI units or 0.125 kgf.s².m⁻⁴, where 1 kgf = 1 kg x 9.81 m/s²).

Appendix C shows plots of $F(k)$ and $G(k)$. The critical value of k corresponding to the critical velocity U_c , as far as suspension bridges are concerned, lies below 1. Therefore, (see Appendix C) presents $F(k)$ and $G(k)$, $J_0=\text{BESSELJ}(k,0)$, $J_1=\text{BESSELJ}(k,1)$, $Y_0=\text{BESSELY}(k,0)$ and $Y_1=\text{BESSELY}(k,1)$, restricted to values $0 \leq k \leq 1$.

The equations of motion of the vibrating plate are, considering self-excited forces:

$$m\ddot{h} + c_h\dot{h} + k_h h = -L \quad (2.7)$$

$$I_\alpha\ddot{\alpha} + c_\alpha\dot{\alpha} + k_\alpha \alpha = M \quad (2.8)$$

where

m = mass of bridge deck by unit length;

I_α = polar mass moment of inertia by unit length;

$c_h, c_\alpha, k_h, k_\alpha$ = damping and stiffness coefficients.

h, α = heaving and pitching modes, respectively.

Various forms for the linear expressions for L and M have been employed. The classic theoretical (and some experimental) work has used complex number forms based on the representation of the flutter oscillation as having the complex form $e^{i\omega t}$, as for example Klöppel [28], [29], [30] and Starossek [76], [80]. In the United States, real forms have been preferred, as stated by Scanlan [67]. A new representation convention is also suggested by Zasso [104]. The real and complex number forms will be presented next.

Considering solutions of the type $e^{i\omega t}$, equations (2.7) and (2.8) read:

$$h = h_0 e^{i\omega t} \quad (2.9)$$

$$\alpha = \alpha_0 e^{i(\omega t + \varphi)} \quad (2.10)$$

The following expressions are derived from equations (2.9) and (2.10):

$$\dot{h} = i\omega h; \quad i\dot{h} = -\omega h; \quad \dot{h}/\omega = ih \quad (2.11)$$

$$\dot{\alpha} = i\omega \alpha; \quad i\dot{\alpha} = -\omega \alpha; \quad \dot{\alpha}/\omega = i\alpha \quad (2.12)$$

$$\ddot{h} = -\omega^2 h \quad (2.13)$$

$$\ddot{\alpha} = -\omega^2 \alpha \quad (2.14)$$

Substituting equations (2.13) and (2.14) in (2.3) and (2.4), one obtains:

$$\mathbf{F}_L = \begin{bmatrix} -L \\ M \end{bmatrix} = \begin{bmatrix} \pi \rho b^2 (U \dot{\alpha} - \omega^2 h) + 2 \pi \rho U b (F(k) + i G(k)) (U \alpha + \dot{h} + b \dot{\alpha} / 2) \\ \pi \rho b^2 (b U \dot{\alpha} / 2 - b^2 \omega^2 \alpha / 8) + \pi \rho U b^2 (F(k) + i G(k)) (U \alpha + \dot{h} + b \dot{\alpha} / 2) \end{bmatrix} \quad (2.15)$$

2.3. Notation of the unsteady forces according to Scanlan

The imaginary components of the matrix \mathbf{F}_L are transformed in real numbers if $i\dot{h}$ is substituted by \dot{h}/ω ; $i\alpha$ is substituted by α/ω ; $i\dot{h}$ is substituted by $-\omega h$ and $i\alpha$ is substituted by $-\omega \alpha$ in equations (2.15). The result is

$$\mathbf{F}_L = \begin{bmatrix} -L \\ M \end{bmatrix} = \begin{bmatrix} \pi \rho b^2 (U \dot{\alpha} - \omega^2 h) + 2 \pi \rho U b F(k) (U \alpha + \dot{h} + b \dot{\alpha} / 2) \\ \quad + 2 \pi \rho U b G(k) (U \dot{\alpha} / \omega - \omega h - b \omega \alpha / 2) \\ \pi \rho b^2 (b U \dot{\alpha} / 2 - b^2 \omega^2 \alpha / 8) + \pi \rho U b^2 F(k) (U \alpha + \dot{h} + b \dot{\alpha} / 2) \\ \quad + \pi \rho U b^2 G(k) (U \dot{\alpha} / \omega - \omega h - b \omega \alpha / 2) \end{bmatrix} \quad (2.16)$$

The right-hand terms of equations (2.16) corresponding to L and M are all real numbers.

The terms in \dot{h} in the upper part of (2.16) read:

$$\begin{aligned} 2 \pi \rho U b F(k) \dot{h} &= 2 \pi \rho \frac{U^2}{2} 2 b F(k) \dot{h} / U = \rho U^2 2 b (2 k / 4) (2 \pi F(k) / k) \dot{h} / U = \\ &= \rho U^2 (B K / 4) (2 \pi F(k) / k) \dot{h} / U = \rho U^2 B [K H_1^*(k) \dot{h} / U] \end{aligned}$$

where

$$H_1^*(k) = 2 \pi F(k) / k \quad (2.17)$$

The terms in α in the upper part of (2.16) read:

$$\begin{aligned} \pi \rho b^2 (U \dot{\alpha}) + 2 \pi \rho U b F(k) b \dot{\alpha} / 2 + 2 \pi \rho U b G(k) (U \dot{\alpha} / \omega) &= \\ = \rho U^2 2 b (2 k / 8) [1 + 2 G(k) / k + F(k)] B \dot{\alpha} / U &= \rho U^2 B K H_2^*(k) B \dot{\alpha} / U \end{aligned}$$

where

$$H_2^*(k) = (\pi / 8 k) [1 + 2 G(k) / k + F(k)] \quad (2.18)$$

The terms in α in the upper part of (2.16) read:

$$1/2 \rho U^2 2 b k^2 8 [F(k) - k G(k) / 2] (2 \pi / 8 k^2) \alpha = \rho U^2 2 b K^2 H_3^*(k) \alpha$$

where

$$H_3^*(k) = (2\pi/8k^2)[F(k) - kG(k)/2] \quad (2.19)$$

The terms in h/b in the upper part of (2.16) read:

$$\pi\rho b^2 \omega^2 h + 2\pi\rho U b G(k) \omega h$$

$$1/2 \rho U^2 2b (K^2/4)[1/2 + G(k)/k] 2\pi (h/b)] = \rho U^2 2b K^2 H_4^*(k) (h/b)$$

where

$$H_4^*(k) = -2\pi [1/8 + G(k)/4k] \quad (2.20)$$

The upper part of (2.16) can be written with real numbers as:

$$-L = \rho U^2 B [KH_1^*(k) \dot{h}/U + KH_2^*(k) B\dot{\alpha}/U + K^2 H_3^*(k) \alpha + K^2 H_4^*(k) h/B] \quad (2.21a)$$

The lower part of (2.16) can be represented similarly as:

$$M = \rho U^2 B^2 [KA_1^*(k) \dot{h}/U + KA_2^*(k) B\dot{\alpha}/U + K^2 A_3^*(k) \alpha + K^2 A_4^*(k) h/B] \quad (2.21b)$$

where

$$A_1^*(k) = \pi F(k)/8k \quad (2.22)$$

$$A_2^*(k) = (\pi/32k) [F(k) - 1 + 2G(k)/k] \quad (2.23)$$

$$A_3^*(k) = (\pi/16k^2)[F(k) - kG(k)/2 + k^2/8] \quad (2.24)$$

$$A_4^*(k) = -\pi G(k)/8k \quad (2.25)$$

The real terms $H_{i=1,3}^*$ and $A_{i=1,3}^*$ were introduced by Scanlan & Tomko [66] , who neglected terms in h and intentionally omitted air inertial terms in \ddot{h} and $\ddot{\alpha}$. Terms with coefficients H_4^* and A_4^* are added herein for completeness. All these formulae can be found in Scanlan et al. in [62], where L and M are expressed as functions of k instead of K and b , instead of B . In this case, the full expressions for L , M , $H_{i=1,4}^\#$ and $A_{i=1,4}^\#$ are (as shown in [62]):

$$-L = \frac{1}{2} \rho U^2 2b [kH_1^\#(k) \dot{h}/U + kH_2^\#(k) b\dot{\alpha}/U + k^2 H_3^\#(k) \alpha + k^2 H_4^\#(k) h/B]$$

$$M = \frac{1}{2} \rho U^2 2b^2 [kA_1^\#(k) \dot{h}/U + kA_2^\#(k) b\dot{\alpha}/U + k^2 A_3^\#(k) \alpha + k^2 A_4^\#(k) h/b]$$

where

$$H_1^\#(k) = 2\pi F(k)/k \quad A_1^\#(k) = \pi F(k)/k$$

$$H_2^\#(k) = (\pi/k) [1 + 2G(k)/k + F(k)]; \quad A_2^\#(k) = (\pi/2k) [F(k) - 1 + 2G(k)/k]$$

$$H_3^\#(k) = (2\pi/k^2)[F(k) - kG(k)/2]; \quad A_3^\#(k) = (\pi/k^2) [F(k) - kG(k)/2 + k^2/8]$$

$$H_4^{\#}(k) = -2\pi [1/2 + G(k)/k] \quad A_4^{\#}(k) = -\pi G(k)/k$$

Expressions $H_{i=1,4}^*$ [(2.17) to (2.20)] and $A_{i=1,4}^*$ [(2.22) to (2.25)] versus k are shown in Table 2-1:

K	k	H*1= 2πF/4k	H*2= π(1+F+2G/k)/8k	H*3= 2π(F-kG/2)/8k ²	H*4= =-0.25*π*(1+2*G/k)	A*1= πF/8k	A*2= K3-π(1-F-2G/k)/32k	A*3= π(F-kG/2+k*2/8)/16k ²	A*4= =-0.125*π*G/k
0	0	1.5708E+05	-8.3476E+05	7.8539E+09	17.4806	3.9269E+04	-2.2833E+05	1.9635E+09	4.5665E+00
0.2	0.1	13.0678	-6.3386	66.0158	1.9211	3.2670	-3.5482	16.5285	0.6766
0.4	0.2	5.7144	-0.3115	14.6564	0.6961	1.4286	-1.0596	3.6886	0.3704
0.6	0.3	3.4818	0.6146	6.0377	0.1535	0.8704	-0.5009	1.5340	0.2347
0.8	0.4	2.4543	0.7855	3.2298	-0.1375	0.6136	-0.2945	0.8320	0.1620
1	0.5	1.8785	0.7815	1.9968	-0.3119	0.4696	-0.1973	0.5238	0.1184
1.2	0.6	1.5153	0.7327	1.3529	-0.4247	0.3788	-0.1441	0.3628	0.0902
1.4	0.7	1.2673	0.6752	0.9761	-0.5017	0.3168	-0.1117	0.2686	0.0709
1.6	0.8	1.0881	0.6199	0.7372	-0.5566	0.2720	-0.0905	0.2089	0.0572
1.8	0.9	0.9528	0.5700	0.5764	-0.5972	0.2382	-0.0757	0.1686	0.0471
2	1	0.8473	0.5258	0.4630	-0.6279	0.2118	-0.0649	0.1403	0.0394

Table 2-1 - Aerodynamic derivatives $H_{i=1,4}^*$ and $A_{i=1,4}^*$, considering the aerodynamic mass

2.4. Notation of the unsteady forces according to Klöppel

According to Klöppel & Thiele [28] and following Starossek [80], the air force vector F_L is given by:

$$F_L = \begin{bmatrix} L \\ M \end{bmatrix} = \frac{1}{2} \rho U^2 2\pi k^2 \begin{bmatrix} c_{hh} & b c_{h\alpha} \\ b c_{\alpha h} & b^2 c_{\alpha\alpha} \end{bmatrix} \begin{bmatrix} h \\ \alpha \end{bmatrix} \quad (2.26)$$

The air force coefficients, or aerodynamic derivatives, are complex and are given by:

$$\begin{aligned} c_{hh}(k) &= 1 - (2i/k) C(k) ; c_{h\alpha}(k) = (-1/k) [i(C(k) + 1) + (2/k)C(k)] \\ c_{\alpha h}(k) &= (i/k) C(k) ; c_{\alpha\alpha}(k) = (1/2k) (C(k) - 1) + (1/k^2)C(k) + 1/8 \end{aligned} \quad (2.27), (2.28); (2.29), (2.30)$$

Substituting $C(k) = F(k) + iG(k)$ in the equations above, one obtains:

$$\begin{aligned} c_{hh}(k) &= 1 - (2i/k) (F + iG) = \\ &= (1 + 2G)/k - (2F/k)i = (4/\pi)(H_4^* + H_1^*i) \end{aligned} \quad (2.31)$$

$$\begin{aligned} c_{h\alpha}(k) &= -(1/k) [i(C + 1) + (2/k) C] = \\ &= [(-2/k^2) (F - kG/2)] - [(2/k)((1 + F)/2 + G/k)i] = \\ &= (8/\pi)(H_3^* + H_2^*i) \end{aligned} \quad (2.32)$$

$$\begin{aligned} c_{\alpha h}(k) &= (1/k) C = (1/k) (F + iG) = \\ &= -G/k + (F/k)i = (8/\pi)(A_4^* + A_1^*i) \end{aligned} \quad (2.33)$$

$$c_{\alpha\alpha}(k) = (1/2k)(C - 1) + (1/k^2)C + 1/8 =$$

$$= [(1/k^2)(F - kG/2 + 1/8)] + [(1/k)((F - 1)/2 + G/k)]i =$$

$$= (16/\pi)(A_3^* + A_2^*i) \quad (2.34)$$

Now, if the c'_{ij} and c''_{ij} derivatives are available, it is possible to calculate Scanlan derivatives $H_{i=1,4}^*$ and $A_{i=1,4}^*$ as π -multiples of c'_{ij} and c''_{ij} . The derivatives c'_{ij} and c''_{ij} for a flat plate were taken from Thiesemann [88]. $H_{i=1,4}^*$ and $A_{i=1,4}^*$ were obtained as π -multiples of c'_{ij} and c''_{ij} , compare Table 2-2 and Table 2-3.

Theodorsen (c_{ij} according to Thiesemann, op. cit. , page 266)								
k	c'_{hh}	c''_{hh}	c'_{ah}	c''_{ah}	c'_{ha}	c''_{ha}	c'_{aa}	c''_{aa}
0.1	-2.4460	-16.6400	1.7230	8.3190	-168.1000	16.1400	84.1800	-18.0700
0.2	-0.8862	-7.2760	0.9430	3.6380	-37.3200	0.7933	18.7900	-5.3970
0.3	-0.1955	-4.4330	0.5977	2.2170	-15.3700	-1.5650	7.8120	-2.5510
0.4	0.1751	-3.1250	0.4125	1.5620	-8.2250	-2.0000	4.2370	-1.5000
0.5	0.3972	-2.3920	0.3014	1.1960	-5.0850	-1.9900	2.6670	-1.0050
0.6	0.5407	-1.9290	0.2296	0.9647	-3.4450	-1.8660	1.8480	-0.7337
0.7	0.6338	-1.6140	0.1806	0.8068	-2.4860	-1.7190	1.3680	-0.5689
0.8	0.7087	-1.3850	0.1456	0.6927	-1.8770	-1.5790	1.0640	-0.4607
0.9	0.7603	-1.2130	0.1198	0.6066	-1.4680	-1.4510	0.8589	-0.3854
1	0.7995	-1.0790	0.1003	0.5394	-1.1790	-1.3390	0.7146	-0.3306

Hi, Ai = proporcional to cij								
k	H_4^* = $-\pi/4 \cdot c'_{hh}$	H_1^* = $-\pi/4 \cdot c''_{hh}$	A_4^* = $\pi/8 \cdot c'_{ah}$	A_1^* = $\pi/8 \cdot c''_{ah}$	H_3^* = $-\pi/8 \cdot c'_{ha}$	H_2^* = $-\pi/8 \cdot c''_{ha}$	A_3^* = $\pi/16 \cdot c'_{aa}$	A_2^* = $\pi/16 \cdot c''_{aa}$
0.1	1.9211	13.0690	0.6766	3.2669	66.0127	-6.3382	16.5287	-3.5480
0.2	0.6960	5.7146	0.3703	1.4286	14.6555	-0.3115	3.6894	-1.0597
0.3	0.1535	3.4817	0.2347	0.8706	6.0358	0.6146	1.5339	-0.5009
0.4	-0.1375	2.4544	0.1620	0.6134	3.2299	0.7854	0.8319	-0.2945
0.5	-0.3120	1.8787	0.1184	0.4697	1.9969	0.7815	0.5237	-0.1973
0.6	-0.4247	1.5150	0.0902	0.3788	1.3528	0.7328	0.3629	-0.1441
0.7	-0.4978	1.2676	0.0709	0.3168	0.9762	0.6750	0.2686	-0.1117
0.8	-0.5566	1.0878	0.0572	0.2720	0.7371	0.6201	0.2089	-0.0905
0.9	-0.5971	0.9527	0.0470	0.2382	0.5765	0.5698	0.1686	-0.0757
1	-0.6279	0.8474	0.0394	0.2118	0.4630	0.5258	0.1403	-0.0649

Table 2-2 – Theodorsen derivatives c'_{ij} , c''_{ij} and H_{ij}^* , A_{ij}^* obtained as π - multiples of c'_{ij} .

2.5. Unsteady forces, disregarding the inertia effect of the aerodynamic mass

$$H_4^*(k) = -2\pi [1/8 + G(k)/4k] \quad (2.35a)$$

$$A_3^*(k) = [F(k) - kG(k)/2 + k^2/8] (\pi/16k^2) \quad (2.35b)$$

Are simplified to:

$$H_4^{**}(k) = -2\pi [G(k)/4k] \quad (2.36a)$$

$$A_3^{**}(k) = [F(k) - kG(k)/2](\pi/16k^2) \quad (2.36b)$$

The aerodynamic derivatives of a flat plate neglecting the inertia effect of the aerodynamic mass are displayed in Table 2-3, for $0.05 \leq k \leq 0.5$.

K	k	H*1	H*2	H*3	H**4	A*1	A*2	A**3	A*4
		$=2\pi F/4k$	$=\pi(1+F+2G/k)/8k$	$=2\pi(F-kG/2)/8k^2$	$=-$ $0.25*\pi*(0+2*G/k)$	$=\pi F/8k$	$=-\pi(1-F-2G/k)/32k$	$=\pi(F-kG/2+k^2/8)/16k^2$	$=-0.125*\pi*G/k$
0.1	0.05	28.5574	-26.0498	286.5997	4.1043	7.1393	-10.4394	71.6499	1.0261
0.2	0.1	13.0678	-6.3386	66.0158	2.7065	3.2670	-3.5482	16.5039	0.6766
0.3	0.15	8.0927	-1.8674	27.4638	1.9526	2.0232	-1.7758	6.8659	0.4881
0.4	0.2	5.7144	-0.3115	14.6564	1.4815	1.4286	-1.0596	3.6641	0.3704
0.5	0.25	4.3514	0.3308	8.9939	1.1639	1.0879	-0.7027	2.2485	0.2910
0.6	0.3	3.4818	0.6146	6.0377	0.9389	0.8704	-0.5009	1.5094	0.2347
0.7	0.35	2.8853	0.7386	4.3152	0.7733	0.7213	-0.3764	1.0788	0.1933
0.8	0.4	2.4543	0.7855	3.2298	0.6479	0.6136	-0.2945	0.8075	0.1620
0.9	0.45	2.1301	0.7935	2.5044	0.5505	0.5325	-0.2380	0.6261	0.1376
1	0.5	1.8785	0.7815	1.9968	0.4735	0.4696	-0.1973	0.4992	0.1184

Table 2-3 - Aerodynamic derivatives of a flat plate, neglecting the aerodynamic mass.

2.6. Aerodynamic derivatives of various types of bridge decks

The question of the aerodynamic stability of long-span bridges has been pursued by many researchers, since the dramatic failure of the Tacoma Narrows Bridge in the fall of 1940. In the years 1967 and 1968, Sabzevari & Scanlan [57], [58], [59] developed a theoretical and experimental approach for assessing the aerodynamic (flutter) forces. The method was based on a linearized mathematical model in which the general aerodynamic forces employed were obtained in coefficient forms as functions of the reduced velocity $v = U/N \cdot b$ (U being the velocity of the wind flow, N the frequency and b some characteristic length) from simple wind tunnel tests on bridge deck models.

These wind tunnel tests would be employed to build up a catalog of quantitative characteristics on aerodynamic forces for various box girder cross sections. Such tests, together with those on stiffening truss and girder designs in time could form the basis for calculations of bridge aerodynamic stability without further recourse to the wind tunnel. The same objective was pursued independently by Klöppel et al. [28], [29], [30], in a series of articles from 1963 to 1975. Klöppel wind tests were made in the University of Darmstadt, following the procedures laid down by Barbré & Ibing [2] in 1958, for the Köln-Rodenkirchen suspension bridge. More than 20 different cross sections were investigated regarding their aerodynamic properties.

2.7. Methods of extraction

Two experimental methods using section models have generally been recognized as standard methods for the extraction of flutter derivatives: (1) the use of a free vibration technique and (2) the use of forced oscillation methods. The description of these methods may be found in Thiesemann [88], Sarkar

[68] and Bergmann [4]. The literature about derivative extraction is very extense and can be looked for in the cited doctoral theses or for example in Singh [73] or Zasso et al. [105]. Inter-relations among flutter derivatives is presented by Scanlan et al. [65]. Reports by Starossek [81] and Starossek et al. [75] on flutter derivatives obtained in the hydraulic channel of the University of Hamburg are employed in the present work because they are best fit to our present purposes.

2.8. Thiesemann results

Aerodynamic derivatives of 31 different profiles have been extracted by Thiesemann [88], either experimentally or numerically. The investigated profiles are shown in Table 2-4.

Profile group	Profile	Page	Description, reference
Trapeze-like sections	GB	Page 193	Great Belt Bridge [36, 38]
	B2	Page 195	Great Belt Bridge [36]
	B3	Page 197	Great Belt Bridge [36]
	B4	Page 199	Great Belt Bridge [36]
	B5	Page 201	Great Belt Bridge [36]
	B6	Page 203	Great Belt Bridge [36]
	B7	Page 205	Great Belt Bridge [36]
	B8	Page 207	Trapeze cross section
	M	Page 209	Millau Bridge
	B9	Page 211	Tsurumi Bridge
	B10	Page 213	Tsing-Ma Bridge
	B11	Page 215	Normandie Bridge
	B12	Page 217	Tatara Bridge
	B13	Page 219	Mexico
B14	Page 221	Plate-like Profile	
Trapeze-like sections with guide vanes	S	Page 223	Severn Bridge
	L1	Page 225	Humber Bridge
	L2	Page 227	Jiangyin Bridge
	L3	Page 229	Messina Bridge
Rectangular profiles	R4	Page 231	Rectangle B:H=4:1
	R4	Page 233	Rectangle B:H=8:1
	R16	Page 235	Rectangle B:H=16:1
	R20v	Page 237	Rectangle with a vertical diafragm
	P	Page 239	Rectangle B:H=25:1
	R200	Page 241	Rectangle B:H=200:1
Other profiles	TC	Page 243	Tacoma Bridge
	T2	Page 245	Tacoma H:B=1:10
	C	Page 247	Chongqing Bridge
	C2	Page 249	Chongqing variant
	C3	Page 251	Chongqing without wings
	G	Page 253	Gibraltar Bridge [35],[37]

Table 2-4 - List of profiles examined by Thiesemann

2.9. Buffeting forces

The quasi-steady buffeting forces (exclusive of the steady part) due to wind turbulence are, according to Scanlan & Jones [63]:

$$L_b = -\frac{1}{2} \rho U^2 B [C_L (2u/U) + (C'_L + C_D)(w/U)] \quad (2.37)$$

$$M_b = \frac{1}{2} \rho U^2 B^2 [C_M (2u/U) + C'_M (w/U)] \quad (2.38)$$

where C_L and C_M are the mean lift and moment coefficients (referred to deck width B) of a typical deck section; $C'_L = dC_L/d\alpha$ and $C'_M = dC_M/d\alpha$ and $u = u(t)$, $w = w(t)$ are wind horizontal and vertical gust components, respectively. These gust forces neglect self-induced buffeting effects. Primes denote first derivatives with respect to the angle of attack α at $\alpha = 0$. The variables $C'_L = dC_L/d\alpha$ and $C'_M = dC_M/d\alpha$ for $\alpha = 0$ are given by Thiesemann [88] for 31 different profiles. For a completely accurate description, these expressions must be modified by aerodynamic admittance factors according to Davenport [11] and Kumarasena [33].

2.10. Equations of motion of the mechanical system bridge deck - wind

The linear dynamic system of the bridge deck subjected to self-excited and buffeting wind forces is approximated by the following two degrees of freedom equation:

$$m\ddot{h} + c_h \dot{h} + k_h h = -\rho U^2 B [KH_1^*(k) \frac{\dot{h}}{U} + KH_2^*(k) B \frac{\dot{a}}{U} + K^2 H_3^*(k) \alpha + K^2 H_4^{**}(k) \frac{h}{B}] - \frac{1}{2} \rho U^2 B [C_L \frac{2u}{U} + (C'_L + C_D) \frac{w}{U}] \quad (2.39)$$

$$I_\alpha \ddot{\alpha} + c_\alpha \dot{\alpha} + k_\alpha h = \rho U^2 B^2 [KA_1^*(k) \frac{\dot{h}}{U} + KA_2^*(k) B \frac{\dot{a}}{U} + K^2 A_3^{**}(k) \alpha + K^2 A_4^{**}(k) \frac{h}{B} + \frac{1}{2} \rho U^2 B^2] \quad (2.40)$$

Neglecting for the moment the buffeting forces and transforming (2.39) and (2.40) into the Laplace domain with zero initial conditions gives:

$$[ms^2 + c_h s + k_h] \mathcal{L}(h) = -\frac{1}{2} \rho U^2 B [s 2KH_1^*(k) \frac{\mathcal{L}(h)}{U} + s 2KH_2^*(k) B \frac{\mathcal{L}(a)}{U} + 2K^2 H_3^*(k) \mathcal{L}(a) + 2K^2 H_4^{**}(k) \frac{\mathcal{L}(h)}{B}] \quad (2.41)$$

$$[I_\alpha s^2 + c_\alpha s + k_\alpha] \mathcal{L}(\alpha) = \frac{1}{2} \rho U^2 B^2 \left[s 2K A_1^*(k) \frac{\mathcal{L}(h)}{U} + s 2K A_2^*(k) B \frac{\mathcal{L}(\alpha)}{U} + 2K^2 A_3^{**}(k) \mathcal{L}(\alpha) + 2K^2 A_4^{**}(k) \frac{\mathcal{L}(h)}{B} \right] \quad (2.42)$$

Substituting the dimensionless Laplace variable $p = s \frac{B}{U}$ in the above equations gives:

$$\left[mB p^2 \frac{U^2}{B^2} + c_h B p \frac{U}{B} + k_h B \right] \mathcal{L}\left(\frac{h}{B}\right) = -\frac{1}{2} \rho U^2 B \left[2K H_1^*(k) p \mathcal{L}\left(\frac{h}{B}\right) + 2K H_2^*(k) p \mathcal{L}(\alpha) + 2K^2 H_3^*(k) \mathcal{L}(\alpha) + 2K^2 H_4^{**}(k) \mathcal{L}\left(\frac{h}{B}\right) \right] \quad (2.43)$$

$$\left[I_\alpha p^2 \frac{U^2}{B^2} + c_\alpha p \frac{U}{B} + k_\alpha \right] \mathcal{L}(\alpha) = \frac{1}{2} \rho U^2 B^2 \left[2K A_1^*(k) p \mathcal{L}\left(\frac{h}{B}\right) + 2K A_2^*(k) p \mathcal{L}(\alpha) + 2K^2 A_3^{**}(k) \mathcal{L}(\alpha) + 2K^2 A_4^*(k) \mathcal{L}\left(\frac{h}{B}\right) \right] \quad (2.44)$$

Equations (2.43) and (2.44) may be written as:

$$\left\{ \begin{bmatrix} mB & 0 \\ 0 & I_\alpha \end{bmatrix} p^2 \frac{U^2}{B^2} + \begin{bmatrix} c_h B & 0 \\ 0 & c_\alpha \end{bmatrix} p \frac{U}{B} + \begin{bmatrix} k_h & 0 \\ 0 & k_\alpha \end{bmatrix} \right\} \begin{bmatrix} \mathcal{L}\left(\frac{h}{B}\right) \\ \mathcal{L}(\alpha) \end{bmatrix} = \begin{bmatrix} Q_{11} & Q_{12} \\ Q_{13} & Q_{14} \end{bmatrix} \begin{bmatrix} \mathcal{L}\left(\frac{h}{B}\right) \\ \mathcal{L}(\alpha) \end{bmatrix} \quad (2.45)$$

Or, in matrix form:

$$\left[\mathbf{M} p^2 \frac{U^2}{B^2} + \mathbf{C} p \frac{U}{B} + \mathbf{K} \right] \mathcal{L}(\mathbf{q}) = [\mathbf{V}_f] [\mathbf{Q}] U^2 \mathcal{L}(\mathbf{q}) \quad (2.46)$$

The matrices that compose equations (2.46) are :

$$\mathbf{q} = \begin{bmatrix} h/B \\ \alpha \end{bmatrix} \quad (2.47)$$

$$\mathbf{V}_f = \begin{bmatrix} -1/2 \rho B & 0 \\ 0 & 1/2 \rho B^2 \end{bmatrix} \quad (2.48)$$

$$\mathbf{M} = \begin{bmatrix} mB & 0 \\ 0 & I_\alpha \end{bmatrix} ; \quad \mathbf{C} = \begin{bmatrix} c_h B & 0 \\ 0 & c_\alpha \end{bmatrix} ; \quad \mathbf{K} = \begin{bmatrix} k_h & 0 \\ 0 & k_\alpha \end{bmatrix} \quad (2.49)$$

$$\mathbf{Q} = \begin{bmatrix} 2K^2 H_4^{**} + p 2KH_1^* & 2K^2 H_3^* + p 2KH_2^* \\ 2K^2 A_4^* + p 2KA_1^* & 2K^2 A_3^{**} + p 2KA_2^* \end{bmatrix} \quad (2.50)$$

The unsteady aerodynamic data \mathbf{Q} , obtained from experiments or through Theodorsen functions are determined only for purely imaginary terms of the dimensionless Laplace variable $p = iK$. Thus, the approximation is performed for

oscillatory motion only. The unsteady aerodynamics are described by (2.50) for $p = iK$. Hence,

$$\mathbf{Q} = \begin{bmatrix} 2K^2 H_4^{**} + 2K^2 H_1^* i & 2K^2 H_3^* + 2K^2 H_2^* i \\ 2K^2 A_4^* + 2K^2 A_1^* i & 2K^2 A_3^{**} + 2K^2 A_2^* i \end{bmatrix} \quad (2.51)$$

Note that H_4^{**} and A_3^{**} neglect the inertia effects of the aerodynamic mass.

2.11. Graphs of the aerodynamic data

In order to obtain solutions on the Laplace domain for both growing and decaying motion it is necessary to express the forces as functions of p in the entire non-dimensionalized complex p -plane. The concept of analytic continuation is often used, by extending these functions to the entire complex plane. Analytic functions agreeing with the aerodynamic forcing function at all values of frequency are then sought, see Edwards [13].

The unsteady aerodynamic data are computed for each reduced frequency. For the flat plate, see Table 2-5. Plots of Table 2-5 are shown in Figure 2-2.

K	k	Q_{11r} $=2K^2 H_4^{**}$	Q_{11i} $=2K^2 H_1^{**}$	Q_{12r} $=2K^2 H_3^{**}$	Q_{12i} $=2K^2 H_2^{**}$	Q_{21r} $=2K^2 A_4^{**}$	Q_{21i} $=2K^2 A_1^{**}$	Q_{22r} $=2K^2 A_3^{**}$	Q_{22i} $=2K^2 A_2^{**}$
0.1	0.05	0.0821	0.5711	5.7320	-0.5210	0.0205	0.1428	1.4330	-0.2088
0.2	0.1	0.2165	1.0454	5.2813	-0.5071	0.0541	0.2614	1.3203	-0.2839
0.3	0.15	0.3515	1.4567	4.9435	-0.3361	0.0879	0.3642	1.2359	-0.3197
0.4	0.2	0.4741	1.8286	4.6900	-0.0997	0.1185	0.4572	1.1725	-0.3391
0.5	0.25	0.5820	2.1757	4.4969	0.1654	0.1455	0.5439	1.1242	-0.3514
0.6	0.3	0.6760	2.5069	4.3471	0.4425	0.1690	0.6267	1.0868	-0.3606
0.7	0.35	0.7579	2.8276	4.2289	0.7238	0.1895	0.7069	1.0572	-0.3688
0.8	0.4	0.8293	3.1415	4.1342	1.0054	0.2073	0.7854	1.0335	-0.3770
0.9	0.45	0.8919	3.4507	4.0571	1.2854	0.2230	0.8627	1.0143	-0.3855
1	0.5	0.9469	3.7569	3.9937	1.5631	0.2367	0.9392	0.9984	-0.3946

Table 2-5- Unsteady aerodynamic data for a flat plate, $0.05 \leq k \leq 0.5$

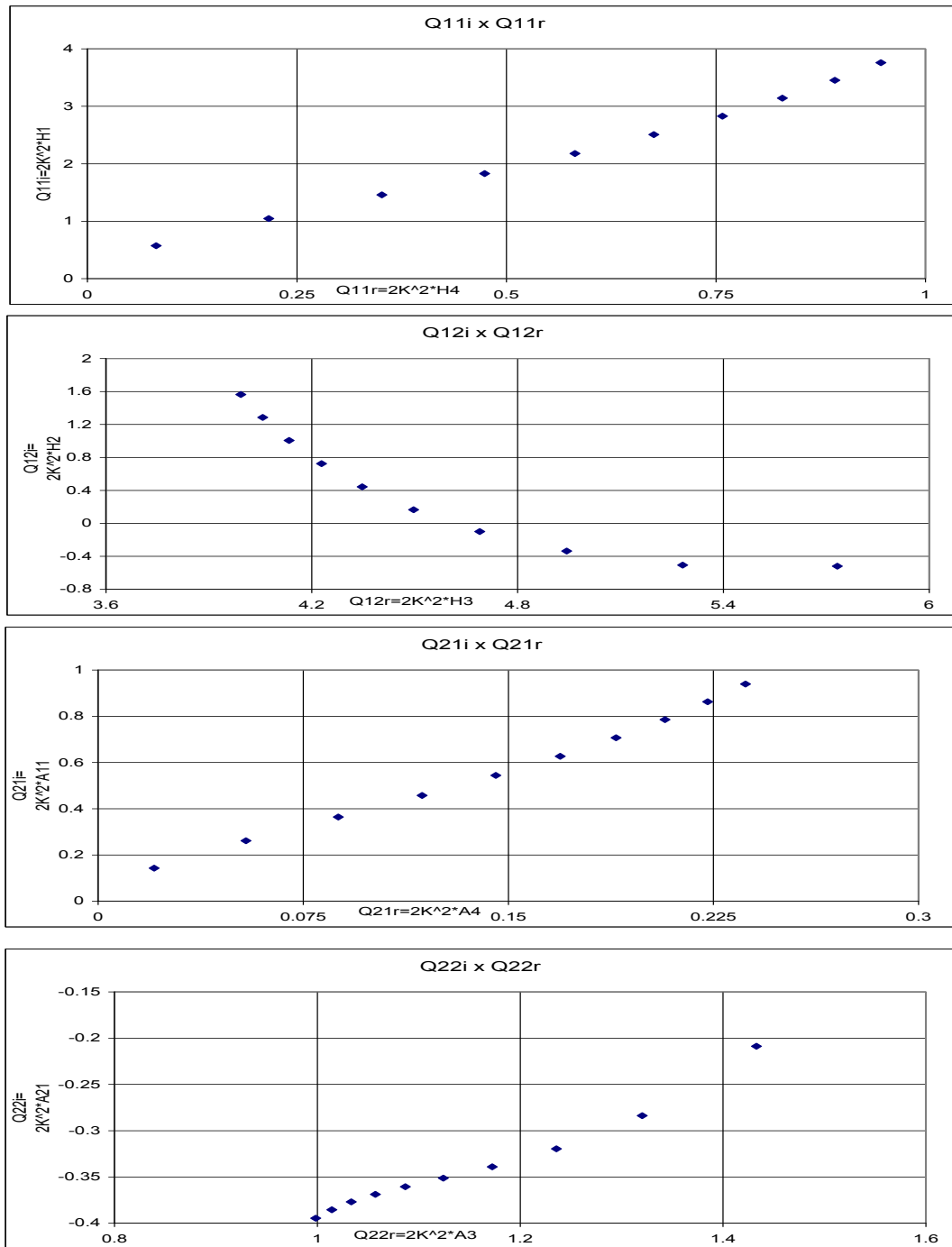


Figure 2-2 - Unsteady aerodynamic data corresponding to Table 2-5